SUPPLEMENTARY INFORMATION:
Temperature-dependence of graphene stress and elasticity

Roberto De Alba, T. S. Abhilash, and Jeevak M. Parpia
Department of Physics, Cornell University, Ithaca NY, 14853, USA

Aaron Hui and Harold G. Craighead
School of Applied and Engineering Physics, Cornell University, Ithaca NY, 14853, USA

CONTENTS

S1. EFFECT OF INCLUDING 3 PARAMETERS IN THE LOW-TEMPERATURE FITS

As discussed in the main text, fits to the resonant frequency ω_0 versus gate voltage V_{dc} become increasingly difficult to perform at low temperatures, where the membrane tension σ_0 increases significantly and the effect of V_{dc} on ω_0 is therefore reduced. It was thus determined that in order to extract meaningful results from the fits, the membrane mass density ρ should be constrained to its fitted value at 300 K. Figure S1 shows the results of fits to the low temperature data (Figs. 3 (a) & 4 (a)) in which the mass was not constrained. These should be compared to Figs. 3 (b) & 4 (b) of the main text, in which ρ was constrained.

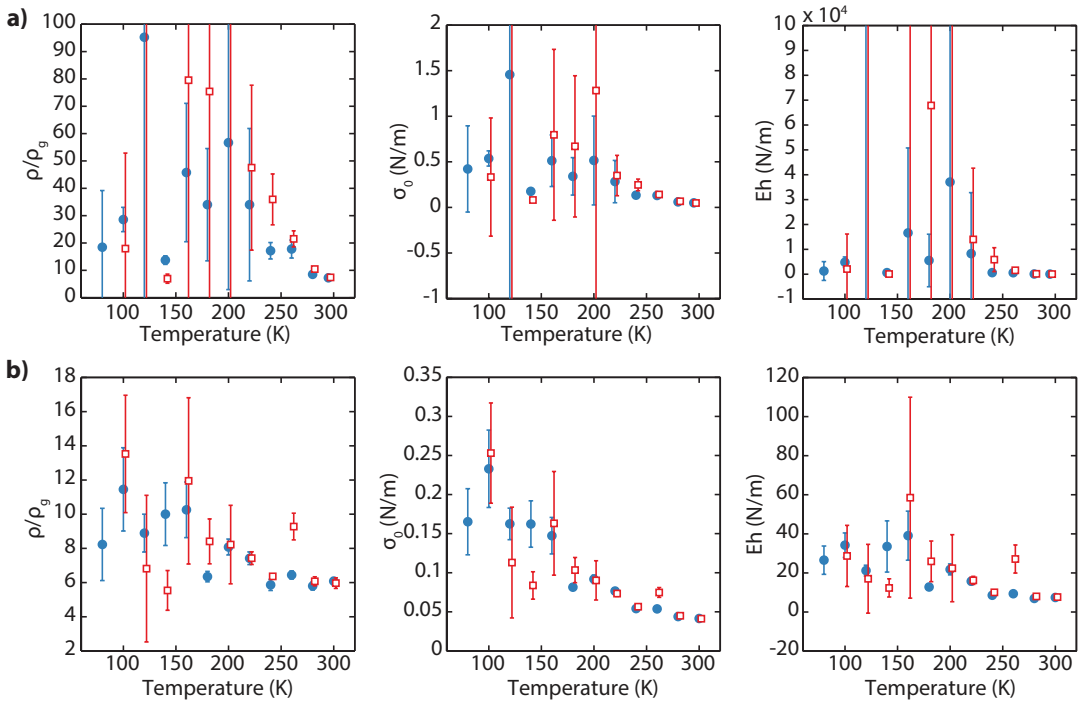

FIG. S1. **Results of 3-parameter fits.** Mass density ρ (in units of ρ_g, the density of monolayer graphene), built-in tension σ_0, and modulus Eh versus temperature for (a) Device 1 and (b) Device 2. Blue circles: values measured during cooling to 80 K. Red squares: values measured during heating to 300 K

S2. EXTRACTING RESONANT FREQUENCY & QUALITY FACTOR FROM A DUFFING LINESHAPE

In order to obtain resonant frequencies and quality factors from nonlinear lineshapes – such as that shown in Figure 2c,d of the main article – the graphene membrane is assumed to obey the following equation of motion:

$$\ddot{x} + \gamma\dot{x} + \omega_0^2 x + Dx^3 = \frac{F(t)}{m}. \tag{S1}$$

Above, x denotes the deflection at the membrane center, while γ, ω_0, m denote its damping, resonant frequency, and effective mass (discussed in Section S3 A) respectively. The device quality factor is defined as $Q = \omega_0/\gamma$, and $F(t)$, D are the driving force and Duffing coefficient.

To study the phase and amplitude response $x(t)$ to the drive $F(t)$, it is convenient to use complex variables. Hence we write $F(t) = \tilde{F}e^{i\omega t}$, where ω is the drive frequency and $\tilde{F}$ is a complex scalar; we then assume harmonic motion of the form $x(t) = \tilde{x}e^{i\omega t}$. Using these definitions and referencing a text on nonlinear dynamics (e.g. Ref. 1), we see that for drive frequencies ω near the resonance ω_0, and $Q >> 1$, Equation S1 leads to:

$$\tilde{x} = \frac{\tilde{F}/(2m\omega_0)}{\omega_0 + \frac{3D}{8\omega_0}|\tilde{x}|^2 - \omega + i\gamma/2}. \tag{S2}$$

Written in terms of the peak amplitude $\tilde{A} = -i\tilde{F}/(m\omega\gamma)$, this becomes:

$$\tilde{x} = \frac{\tilde{A}i\gamma/2}{\omega_0 + \frac{3D}{8\omega_0}|\tilde{x}|^2 - \omega + i\gamma/2}. \tag{S3}$$

Multiplying this equation by its complex conjugate shows that the vibration amplitude $|\tilde{x}|$ satisfies the following polynomial:

$$|\tilde{x}|^6\frac{9D^2}{64\omega_0^2} + |\tilde{x}|^4\frac{3D(\omega_0-\omega)}{4\omega_0} + |\tilde{x}|^2\left[(\omega_0-\omega)^2 + \frac{\gamma^2}{4}\right] - \frac{|\tilde{A}|^2\gamma^2}{4} = 0. \tag{S4}$$

Because the above result is cubic in $|\tilde{x}|^2$, it can have at most three real solutions. Indeed, is well known that Duffing oscillators have a critical amplitude $|\tilde{A}|_{\text{crit}}$ above which the resonance peak leans over and becomes multivalued, leading to hysteretic frequency sweeps through the resonance. For $|\tilde{A}| \leq |\tilde{A}|_{\text{crit}}$, Equation S4 gives a single real value for $|\tilde{x}|$; for $|\tilde{A}| > |\tilde{A}|_{\text{crit}}$, it gives three real solutions – the median of which represents unstable behavior and is typically not observed experimentally.

Throughout this work, resonance peaks (like the one shown in Figure 2c,d of the main text) were fitted as follows:

1. Arrange the data as a vector of real frequency values $[\omega_1, \omega_2, \ldots, \omega_N]$, and a vector of complex amplitude values $[\tilde{x}_1, \tilde{x}_2, \ldots, \tilde{x}_N]$. The vector of $\tilde{x} = |\tilde{x}|e^{i\phi}$ values thus contains both amplitude $|\tilde{x}|$ and phase ϕ information as measured by the lock-in amplifier.

2. For a given set of parameters $(\omega, \omega_0, \gamma, D, \tilde{A})$, first numerically solve Equation S4 to determine the fitted amplitude $|\tilde{x}|$. If this equation has multiple real solutions, choose the largest value (since we are interested in the upper branch of Duffing curves – i.e. since we have right-leaning resonance peaks and our frequency sweeps were performed in the upward direction).

3. Substitute this result into Equation S3 to determine the phase of $\tilde{x}$.

4. Iterate this algorithm through each element of the ω and $\tilde{x}$ data vectors. It is important to use an implementation of nonlinear least-squares fitting that can handle complex data. If one is not available, a simple work-around is to rearrange the $1 \times N$ vector of complex values $[\tilde{x}_1, \tilde{x}_2, \ldots, \tilde{x}_N]$ into a $1 \times 2N$ vector of real values such as $[\text{real}(\tilde{x}_1), \text{real}(\tilde{x}_2), \ldots, \text{real}(\tilde{x}_N), \text{imag}(\tilde{x}_1), \text{imag}(\tilde{x}_2), \ldots, \text{imag}(\tilde{x}_N)]$. In this case, the accompanying frequency vector would be $[\omega_1, \omega_2, \ldots, \omega_N, \omega_1, \omega_2, \ldots, \omega_N]$

We note that in the algorithm described above, $\tilde{x}$ has units of volts generated by our high-speed photodetector. The optical transduction scheme is assumed to operate in the linear regime – that is to say device motion is assumed to be much smaller than the 633 nm laser wavelength used. In previous experiments (Ref. 2), we have shown that this condition is easily satisfied. Throughout the remainder of this document, the variable x has units of length.

S3. MODELING THE MEMBRANE FREQUENCY VS GATE VOLTAGE

A. Calculating the resonant frequency of a nonlinear tensioned membrane

As described in Ref. 2, the Lagrangian of a tensioned membrane under electroscatic loading is:

$$\begin{aligned} L = &\frac{\rho}{2}\int dA\dot{x}^2 - \frac{D}{2}\int dA(\Delta x)^2 - \frac{C}{16}\left[\frac{1}{A}\int dA(\nabla x)^2\right]\cdot\int dA(\nabla x)^2 \\ &- \frac{\sigma_0}{2}\int dA(\nabla x)^2 + \frac{\epsilon_0 V_{dc}^2}{2}\int\frac{dA}{d-x} \end{aligned} \tag{S5}$$

where each integral is over the membrane surface area A, x is the membrane's out-of-plane deformation, ρ is the surface density, $D = Yh^3/(12(1-\nu^2))$ and $C = Yh/(1-\nu^2)$ are the bending stiffness and tensile stiffness, σ_0 is the built-in tension, V_{dc} is the applied gate voltage, and d is the gate-membrane separation. Y and ν are the Young's modulus and Poisson ratio, respectively, and h is the membrane thickness. The membrane's out-of-plane deformation $x(\vec{r},t)$ is a function of position $\vec{r}$ and time t, and can be written as a sum of static and oscillating parts:

$$x(\vec{r},t) = x_0\xi_0(\vec{r}) + x_i(t)\xi_i(\vec{r}). \tag{S6}$$

Here we are considering only the motion of a single mechanical eigenmode i. Also, we have introduced x_0 and $x_i(t)$, which represent the deflection at the membrane center (for the static case) and at its antinode (for the oscillating mode). $\xi_0(\vec{r})$ and $\xi_i(\vec{r})$ describe the shape of the static deformation and of mode i, both normalized such that $0 \leq |\xi(\vec{r})| \leq 1$.

As shown in Ref. 2, expressing the deflection in this way allows us to rewrite the Lagrangian as that of a nonlinear 1-Dimensional harmonic oscillator:

$$L = \frac{\rho}{2}\dot{x}_i^2\int dA\xi_i^2 - \frac{\sigma}{2}x_i^2\int dA(\nabla\xi_i)^2 - L_ix_i - S_ix_i^2 - T_ix_i^3 - F_ix_i^4 \tag{S7}$$

where

$$\sigma = \sigma_0 + \frac{Cx_0^2}{4A}\int dA(\nabla\xi_0)^2 \tag{S8}$$

$$L_i = \left[\sigma_0 + \frac{Cx_0^2}{4A}\int dA(\nabla\xi_0)^2\right]\cdot x_0\int dA(\nabla\xi_0\nabla\xi_i) \tag{S9}$$

$$S_i = \frac{Cx_0^2}{4A}\left[\int dA(\nabla\xi_0\nabla\xi_i)\right]^2 \tag{S10}$$

$$T_i = \frac{Cx_0}{4A}\left[\int dA(\nabla\xi_0\nabla\xi_i)\right]\cdot\int dA(\nabla\xi_i)^2 \tag{S11}$$

$$F_i = \frac{C}{16A}\left[\int dA(\nabla\xi_i)^2\right]^2 \tag{S12}$$

Eq. S8 represents the change in membrane tension due to the static deflection x_0. Nonlinearites due to the flexural rigidity D (plate-bending terms) in Eq. S5 have been neglected in Eq. S7 since they scale with $h^2/A \ll 1$. Nonlinear electrostatic terms have been neglected for now, but will be reintroduced in the next section.

The mechanics of mode i can be determined by applying the Euler-Lagrange equation toEq. S7:

$$\frac{d}{dt}\left(\frac{\partial L}{\partial\dot{x}_i}\right) - \frac{\partial L}{\partial x_i} = 0 \tag{S13}$$

which leads to

$$\rho\ddot{x}_i\int dA\xi_i^2 + \sigma x_i\int dA(\nabla\xi_i)^2 + L_i + 2S_ix_i + 3T_ix_i^2 + 4T_ix_i^3 = 0 \tag{S14}$$

Dividing each term above by the effective mass $m_i = \rho\int dA\xi_i^2$ thus produces the familiar harmonic oscillator result:

$$\ddot{x}_i + \omega_i^2 x_i + \{\text{nonlinear terms}\} = 0. \tag{S15}$$

This represents the undamped harmonic oscillator; a phenomenological damping force $\gamma\dot{x}$ is typically added in as well. The resonant frequency of mode i, ω_i, is thus given by:

$$\omega_i = \sqrt{\frac{\sigma \int dA(\nabla\xi_i)^2}{\rho \int dA\xi_i^2}}. \tag{S16}$$

To test this result, we can compare it to the known eigenmodes and eigenfrequencies of circular or square membranes. For circles we know that the mode shape is $\xi_i = \xi_{m,n} = J_m(\frac{\alpha_{m,n}r}{R})\cos(m\theta)$, where (r,θ) are polar coordinates, R is the membrane radius, J_m is the m-th Bessel function and $\alpha_{m,n}$ is its n-th root. For the fundamental mode $(m,n) = (0,1)$, we have $\nabla\xi_i = \frac{d}{dr}J_0\left(\frac{\alpha_{0,1}r}{R}\right) = -\frac{\alpha_{0,1}}{R}\cdot J_1\left(\frac{\alpha_{0,1}r}{R}\right)$. Eq. S16 then gives

$$\omega_{0,1} = \sqrt{\frac{\sigma \int rdr\left(\frac{\alpha_{0,1}}{R}\cdot J_1\left(\frac{\alpha_{0,1}r}{R}\right)\right)^2}{\rho \int rdr\left(J_0\left(\frac{\alpha_{0,1}r}{R}\right)\right)^2}} = \sqrt{\frac{\sigma\left(\frac{\alpha_{0,1}}{R}\right)^2\cdot\frac{1}{2}(J_1(\alpha_{0,1}))^2}{\rho\cdot\frac{1}{2}(J_1(\alpha_{0,1}))^2}} = \frac{\alpha_{0,1}}{R}\sqrt{\frac{\sigma}{\rho}} \tag{S17}$$

where computer algebra software (Ref. 3) was used to evaluate the integrals. This result reproduces the well-known fundamental frequency of a circular drum. Eq. S16 can similarly predict the full spectrum of circular membrane frequencies $\omega_{m,n} = \frac{\alpha_{m,n}}{R}\sqrt{\frac{\sigma}{\rho}}$, however the integration becomes more arduous for a general (m,n). It can likewise be applied to a rectangular membrane $\xi_{m,n} = \sin\left(\frac{m\pi x}{a}\right)\sin\left(\frac{n\pi y}{b}\right)$ to obtain the expected $\omega_{m,n} = \pi\sqrt{\frac{\sigma}{\rho}\left[\left(\frac{m}{a}\right)^2 + \left(\frac{n}{b}\right)^2\right]}$.

The term $\rho\int dA\xi_i^2$ in Eq. S14 is commonly referred to as the effective mass m_i of mode i [4–6], and this concept can be extremely useful when mathematically reducing the 2-dimensional membrane to a 1-dimensional harmonic oscillator (*e.g.* Eq. S15). This 1-dimensional analogy goes so far as to accurately describe the thermal oscillations of x_i. Invoking the equipartition theorem, the time-averaged thermal amplitude $\langle x_i^2(t)\rangle$ is related to the ambient temperature T by:

$$\frac{1}{2}m_i\omega_i^2\langle x_i^2(t)\rangle = \frac{1}{2}k_BT. \tag{S18}$$

Similarly, the quantum zero-point fluctuations of x_i (oscillations expected at $T = 0$) are:

$$\langle x_i^2\rangle_{\text{zpf}} = \frac{\hbar}{2m_i\omega_i}. \tag{S19}$$

Lists of effective masses for several modes of common MEMs geometries (membranes, cantilevers, doubly- clamped bridges) are given in Ref. 4.

B. Contribution of capacitive softening

The electrostatic term in Eq. S5 can be approximated as:

$$\frac{\epsilon_0 V_{dc}^2}{2}\int \frac{dA}{d-x} \approx \frac{\epsilon_0 V_{dc}^2}{2d}\int dA\left(1+\frac{x}{d}+\frac{x^2}{d^2}+\frac{x^3}{d^3}\right) \tag{S20}$$

These terms will play a role in determining the resonant frequency of our membrane as well as its nonlinear coefficients. In order to incorporate these terms into our model, we must substitute $x = x_0\xi_0 + x_i\xi_i$ into Eq. S20 and collect terms in powers of x_i. Once this is done, application of the Euler-Lagrange equation to Eq. S7 gives the following equation of motion:

$$\ddot{x}_i + \gamma_i\dot{x}_i + \left(\omega_i^2 + \frac{2\mathcal{S}_i}{m_i}\right)x_i + \frac{\mathcal{L}_i}{m_i} + \frac{3\mathcal{T}_i}{m_i}x_i^2 + \frac{4\mathcal{F}_i}{m_i}x_i^3 = 0 \tag{S21}$$

where the coefficients $\mathcal{L}_i, \mathcal{S}_i, \mathcal{T}_i, \mathcal{F}_i$ are a sum of the tension-based terms (Eqs. S9-S12) and the electrostatic terms given by Eq. S20. Thus we now have:

$$\mathcal{L}_i = \left(\sigma_0 + \frac{Cx_0^2}{4A}\mathbb{I}_{00}\right)x_0\mathbb{I}_{0i} - \frac{\epsilon_0 V_{dc}^2 A}{2d^2}\left[\mathbb{K}_i + \frac{x_0}{d}2\mathbb{K}_{0i} + \frac{x_0^2}{d^2}3\mathbb{K}_{00i} + \frac{x_0^3}{d^3}4\mathbb{K}_{000i}\right] \tag{S22}$$

$$\mathcal{S}_i = \frac{Cx_0^2}{4A}\mathbb{I}_{0i}^2 - \frac{\epsilon_0 V_{dc}^2 A}{2d^3}\left[\mathbb{K}_{ii} + \frac{x_0}{d}3\mathbb{K}_{0ii} + \frac{x_0^2}{d^2}6\mathbb{K}_{00ii}\right] \tag{S23}$$

$$\mathcal{T}_i = \frac{Cx_0}{4A}\mathbb{I}_{0i}\mathbb{I}_{ii} - \frac{\epsilon_0 V_{dc}^2 A}{2d^4}\left[\mathbb{K}_{iii} + \frac{x_0}{d}4\mathbb{K}_{0iii}\right] \tag{S24}$$

$$\mathcal{F}_i = \frac{C}{16A}\mathbb{I}_{ii}^2 - \frac{\epsilon_0 V_{dc}^2 A}{2d^5}\mathbb{K}_{iiii} \tag{S25}$$

$$\omega_i^2 = \frac{1}{m_i}\left(\sigma_0 + \frac{Cx_0^2}{4A}\mathbb{I}_{00}\right)\mathbb{I}_{ii} \tag{S26}$$

$$m_i = \rho A\mathbb{K}_{ii} \tag{S27}$$

where we have introduced the symbols $\mathbb{I}_{mn}$ and $\mathbb{K}_{jklm}$. These are a set of dimensionless constants (different for each eigenmode) that are determined by solving the integrals $\mathbb{I}_{mn} = \int dA(\nabla\xi_m\nabla\xi_n)$ and $\mathbb{K}_{jklm} = (1/A)\int dA\xi_j\xi_k\xi_l\xi_m$. The full set of these integrals (to 3$^{\text{rd}}$ order in x_0/d) are given in Section S3 E for the fundamental mode of a circular membrane.

Based on Eq. S21, the resonant frequency Ω_i of our membrane is given by $\Omega_i^2 = \omega_i^2 + 2\mathcal{S}_i/m_i$. Furthermore, we have Duffing coefficients given by the cubic restoring force $(4\mathcal{F}_i/m_i)x_i^3$ and quadratic restoring force $(3\mathcal{T}_i/m_i)x_i^2$. And Eqs. S22 - S27 tell us precisely how each of these terms depends on the membrane modulus C, static displacement x_0, and gate voltage V_{dc}. Another added layer of complexity would be to calculate how the constant force $\mathcal{L}_i$ in Eq. S21 affects the equilibrium position of x_i, which would in turn slightly change the resonant frequency because of the nonlinear stiffening terms $\mathcal{T}_i$ and $\mathcal{F}_i$. This turns out to be a small correction to the resonant frequency Ω_i, and can be neglected.

The only remaining piece of the puzzle is to determine the static membrane deflection x_0 as a function of applied gate voltage V_{dc}. This is done in the next section.

C. Static membrane deflection x_0 vs V_{dc}

Our task is now to determine the static deflection of the membrane center x_0 and the static membrane profile ξ_0. One approach is to simply balance the total vertical forces acting on the membrane. Using the parallel-plate capacitor approximation, the force exerted by the gate voltage on the graphene is $F_{dc} = -\epsilon_0 A V_{dc}^2/(2d^2)$. This downward force is balanced all along the circumference of the membrane by an upward tensile force of $F_\sigma = 2\pi R\sigma \sin\theta$, where θ is the contact angle with the substrate. This is depicted schematically in Figure S2.

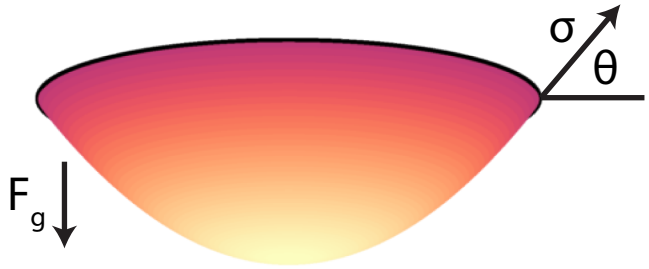

FIG. S2. Balance of forces in the static membrane.

If we approximate the static membrane profile as a paraboloid $\xi_0(r) = 1 - r^2/R^2$ and use a small angle approximation, we can use the simple expression $\sin\theta \approx \tan\theta = (d\xi_0/dr)|_{r=R} = -2x_0/R$. Balance of the upward and downward forces then gives a relation between x_0 and V_{dc}:

$$x_0 = \frac{\epsilon_0 A V_{dc}^2}{8\pi d^2 \sigma} \tag{S28}$$

A second (perhaps more rigorous) approach to calculating x_0 is to consider only static deformation in the original Lagrangian Eq. S5 (*i.e.* to set $x(\vec{r}) = x_0\xi_0(\vec{r})$) and then apply the Euler-Lagrange equation. Because there is no time-dependence, this simplifies to $\partial L/\partial x_0 = 0$. Using Eq. S20 to approximate the electrostatic terms, this approach produces the result

$$-\sigma x_0 \mathbb{I}_{00} + \frac{\epsilon_0 V_{dc}^2 A}{2d^2}\left[\mathbb{K}_0 + \frac{x_0}{d}2\mathbb{K}_{00} + \frac{x_0^2}{d^2}3\mathbb{K}_{000}\right] = 0 \tag{S29}$$

where, as in earlier sections, the total tension is

$$\sigma = \sigma_0 + \frac{C x_0^2}{4A}\mathbb{I}_{00} \tag{S30}$$

In the experimentally relevant limit of $x_0/d \ll 1$, Eq. S29 reduces to

$$x_0 = \frac{\epsilon_0 A V_{dc}^2 \mathbb{K}_0}{2d^2\sigma\mathbb{I}_{00}} \tag{S31}$$

which reproduces Eq. S28 if we use the same approximation of a parabolic membrane shape $\xi_0(r) = 1 - r^2/R^2$ when solving the integrals $\mathbb{I}_{00}$ and $\mathbb{K}_0$. See Section S3 E for numerical values of all the relevant integrals.

D. The final fitting function

Combining the results of Eqs. S21 & S31 (and neglecting terms of order x_0/d and higher) gives the following equation for the resonant frequency of mode i:

$$\Omega_i^2 = \omega_i^2 + \frac{2\mathcal{S}_i}{m_i} \tag{S32}$$

$$= \frac{\mathbb{I}_{ii}\sigma_0}{\mathbb{K}_{ii}\rho A} - \frac{\epsilon_0 V_{dc}^2}{d^3\rho} + \frac{C\epsilon_0^2 V_{dc}^4}{d^4\rho\sigma^2}\frac{\mathbb{K}_0^2(\mathbb{I}_{00}\mathbb{I}_{ii} + 2\mathbb{I}_{0i}^2)}{16\mathbb{K}_{ii}\mathbb{I}_{00}^2} \tag{S33}$$

The various dimensionless integrals $\mathbb{I}$ and $\mathbb{K}$ are given in Section S3 E for the fundamental mode of a circular membrane. If we substitute these numerical values, the above equation becomes

$$\Omega_1^2 = \frac{\alpha^2\sigma_0}{R^2\rho} - \frac{\epsilon_0 V_{dc}^2}{d^3\rho} + \frac{\beta C\epsilon_0^2 V_{dc}^4}{d^4\rho\sigma^2} \tag{S34}$$

where $\alpha = 2.4048$ and $\beta = 0.1316$, reproducing Eq. 1 of the main text. Note that the V_{dc}^4 term above depends on the total tension σ (including electrostatic contributions) rather than the intrinsic tension σ_0. The fitting function used throughout this work was therefore not a simple polynomial, but incorporated Eqs. S30 & S31 to better match the data – particularly at high voltages where σ_0 is no longer a good approximation for σ. Substituting Eq. S31 into Eq. S30 reveals that the total tension is given by the implicit equation

$$\sigma = \sigma_0 + \frac{CR^2\epsilon_0^2 V_{dc}^4}{128 d^4\sigma^2} \tag{S35}$$

where we have used the numerical values of $\mathbb{I}_{00}$ and $\mathbb{K}_0$ given in the next section. The fitting routine employed solved this equation numerically for σ during each iteration of the fit.

We note that simply substituting the total tension σ (Eq S35) into the well-known expression for the resonant frequency of a circular membrane $\omega = (\alpha/R)\sqrt{\sigma/\rho}$ comes close to reproducing the β term in Eq. S34. However, doing so in effect neglects the $\mathcal{S}_i$ term in Eq. S32 (and hence Eq. S21), underestimating β by roughly 70%. This highlights a result of the Lagrangian-based derivation that would otherwise be missed: under the influence of an applied voltage V_{dc}, all eigenmodes of the membrane experience a common tension shift (which traces back to the static deflection ξ_0 in Eq. S8), but each eigenmode also has a unique frequency shift based on its mode shape (ξ_i in Eq. S10).

E. Useful Integrals

The following integrals are helpful when calculating nonlinear contributions to the Lagrangian of a circular tensioned membrane. The static out-of-plane profile is assumed to be quadratic $\xi_0 = 1 - r^2/R^2$, and the first resonant mode is assumed to be a Bessel function $\xi_1 = J_0(\alpha_{0,1} r/R)$.

$$\mathbb{I}_{00} = \int dA (\nabla \xi_0)^2 = 2\pi \tag{S36}$$

$$\mathbb{I}_{11} = \int dA (\nabla \xi_1)^2 = \pi (\alpha_{0,1} J_1(\alpha_{0,1}))^2 \approx \pi \times 1.558650 \tag{S37}$$

$$\mathbb{I}_{01} = \int dA (\nabla \xi_0)(\nabla \xi_1) = \pi 4 J_2(\alpha_{0,1}) \approx \pi \times 1.727019 \tag{S38}$$

$$\mathbb{K}_0 = \frac{1}{A} \int dA \xi_0 = \frac{1}{2} \tag{S39}$$

$$\mathbb{K}_{00} = \frac{1}{A} \int dA (\xi_0)^2 = \frac{1}{3} \tag{S40}$$

$$\mathbb{K}_{000} = \frac{1}{A} \int dA (\xi_0)^3 = \frac{1}{4} \tag{S41}$$

$$\mathbb{K}_1 = \frac{1}{A} \int dA \xi_1 = \frac{2 J_1(\alpha_{0,1})}{\alpha_{0,1}} \approx 0.431755 \tag{S42}$$

$$\mathbb{K}_{11} = \frac{1}{A} \int dA (\xi_1)^2 = (J_1(\alpha_{01}))^2 \approx 0.269514 \tag{S43}$$

$$\mathbb{K}_{111} = \frac{1}{A} \int dA (\xi_1)^3 \approx 0.194923 \tag{S44}$$

$$\mathbb{K}_{01} = \frac{1}{A} \int dA \xi_0 \xi_1 = \frac{4 J_2(\alpha_{0,1})}{(\alpha_{0,1})^2} \approx 0.298628 \tag{S45}$$

$$\mathbb{K}_{001} = \frac{1}{A} \int dA (\xi_0)^2 \xi_1 = \left(\frac{2}{\alpha_{0,1}} \right)^4 (4 J_2(\alpha_{0,1}) - \alpha_{0,1} J_1(\alpha_{0,1})) \approx 0.22894 \tag{S46}$$

$$\mathbb{K}_{011} = \frac{1}{A} \int dA \xi_0 (\xi_1)^2 = \frac{2(1+\alpha_{0,1})^2 (J_1(\alpha_{0,1}))^2}{3\alpha_{0,1}^2} \approx 0.210745 \tag{S47}$$

REFERENCES

[1] A. H. Nayfeh and D. T. Mook, *Nonlinear Oscillations* (Wiley-VCH Verlag GmbH, 2007) pp. 161–257.
[2] R. De Alba, F. Massel, I. R. Storch, T. S. Abhilash, A. Hui, P. L. McEuen, H. G. Craighead, and J. M. Parpia, Nature Nanotechnology **11**, 741 (2016).
[3] *Wolfram Alpha* (Wolfram Alpha LLC, 2016).
[4] B. D. Hauer, C. Doolin, K. S. D. Beach, and J. P. Davis, Annals of Physics **339**, 181 (2013).
[5] M. Aspelmeyer, T. J. Kippenberg, and F. Marquardt, Reviews of Modern Physics **86**, 1391 (2014).
[6] J. P. Cleveland, S. Manne, D. Bocek, and P. K. Hansma, Review of Scientific Instruments **64**, 403 (1993).